SANDIA REPORT
SAND2019-3657
Printed March 2019

Sandia National Laboratories

Empirical Refinement of the GADRAS Detector Response Function

Dean J. Mitchell

Prepared by
Sandia National Laboratories
Albuquerque, New Mexico
87185 and Livermore,
California 94550

Issued by Sandia National Laboratories, operated for the United States Department of Energy by National Technology & Engineering Solutions of Sandia, LLC.

Available to DOE and DOE contractors from
U.S. Department of Energy
Office of Scientific and Technical Information
P.O. Box 62
Oak Ridge, TN 37831

Telephone: (865) 576-8401
Facsimile: (865) 576-5728
E-Mail: reports@osti.gov
Online ordering: http://www.osti.gov/scitech

Available to the public from
U.S. Department of Commerce
National Technical Information Service
5301 Shawnee Rd
Alexandria, VA 22312

Telephone: (800) 553-6847
Facsimile: (703) 605-6900
E-Mail: orders@ntis.gov
Online order: https://classic.ntis.gov/help/order-methods/

ABSTRACT

The Gamma Detector Response and Analysis Software (GADRAS) was augmented to enable empirical refinement of the Detector Response Function (DRF) for gamma-ray detectors. This capability is included in GADRAS starting with Version 18.8.2, which was released in February 2019. Empirical refinement enables improved computational accuracy for gamma-ray spectra when detectors exhibit characteristics that are essentially unique to a particular sensor. This report discusses how to perform the empirical refinement, and examples are presented for the following scenarios where empirical refinement is appropriate:

- Large plastic scintillators, which are generally composed of polyvinyl toluene (PVT), often exhibit low-energy peaks that are not associated with incident gamma rays. Regardless of whether they are artifacts produced by poor light collection or pulse processing methods, accurate spectral synthesis requires replication of these features.
- Some detectors, particularly those using Silicon Photomultipliers (SiPM), exhibit energy shifts of Compton edges and escape peaks relative to the same scintillator material attached to a photomultiplier tube. Empirical refinement compensates for these effects, which derive from nonlinearities in the detector response.
- The change in the DRF as a function of displacement of the source relative to the detector axis cannot always be replicated adequately using only the few shielding parameters that are used by the response function. Empirical refinement enables improved accuracy for computation of spectra during linear transits or when the detector is close to a large radiation source. This is a particularly important consideration for collimated detectors.
- Gamma-ray imagers exhibit complex relationships between spectral response and spatial locations. Empirical refinement enables substantial improvement of the DRF accuracy for imagers.

ACKNOWLEDGEMENTS

This research and development was funded by the Department of Homeland Security (DHS) Counter Weapons of Mass Destruction (CWMD) office and the Department of Energy (DOE), National Nuclear Security Administration (NNSA), Org. NA-22.

CONTENTS

LIST OF FIGURES

ACRONYMS AND DEFINITIONS

Abbreviation	Definition
CsI	Cesium iodide (radiation detector)
CZT	Cadmium zinc telluride (radiation detector)
DRF	Detector Response Function
GADRAS	Gamma Detector Response and Analysis Software
HPGe	High-Purity Germanium (radiation detector)
PVT	Polyvinyl Toluene (radiation detector)
SiPM	Silicon Photomultiplier

1. INTRODUCTION

The Gamma Detector Response and Analysis Software (GADRAS) has been used to compute the response of various types of gamma-ray detectors for more than 30 years. Despite the maturity of the application, the introduction of new types of detectors or more demanding computation requirements necessitates the need for continued improvement. GADRAS Version 18.8.2, which was released in February 2019, includes provisions for empirical refinement of detector response characteristics that are unique to a particular instrument. The general characteristics that are addressed by the empirical refinement procedure are summarized below:

- *Characteristics not directly associated with gamma-ray interaction physics*: In addition to the computation of photopeaks, the Detector Response Function (DRF) replicates scattering of photons into and out of radiation detector materials. Some of the radiation detectors that are of current interest exhibit characteristics that cannot be computed by only tracking gamma-ray interaction probabilities. For example, subtleties associated with light collection in large polyvinyl toluene (PVT) panels that are used in radiation portals produce unusual detector response profiles. Other characteristics that are unique to particular detectors are shifts in the locations of Compton edges and escape peaks, which are produced by nonlinearities in the response. This is particularly important for detectors that are coupled with silicon photomultipliers (SiPM).

- *Angular response*: GADRAS applies a few shielding parameters to approximate the attenuation and scattering of photons through the sides of shielded detectors. These approximations are inadequate for complex configurations, such as radiation portals, which may surround the detector element with varying thicknesses of shielding materials ranging from steel to lead. The demand for greater accuracy in the angular response is even more important for imaging sensors. Simulations for radiation sources as they move through portals are also impacted by the angular response.

This document compares the accuracy of computed spectra based on GADRAS Version 18.8.2 with Version 18.7.9, which was released in April, 2018. The process used to refine the detector response is also described.

2. DETECTOR CHARACTERIZATION METHOD

A reasonable approximation of the response characteristics of gamma-ray detectors can be obtained by specifying the type and size of the detector material. The accuracy of computed spectra is improved by characterizing parameters that represent the energy calibration, detector resolution, and the scatter environment. Data required to achieve this objective consist of measurements of several calibration sources at a fixed distance from the detector. The collection of suitable characterization data is described elsewhere [1], and the process of using GADRAS to adjust response function parameters has also been documented [2].

Although characterization spectra do not need to be contained in a single file, incorporation of all spectra into one file facilitates the process. Figure 1 presents an example of the header information contained in a typical characterization file for a radiation portal. The information following the "@" symbol in the title field declares the distance and optional height from the center of the source to the external face of the radiation detector. The presence of this optional information enables automatic adjustment of these parameters when they change. For example,

all of the calibration sources were measured at 240 cm, but the welding rods (record 6) were measured at 27 cm in this example. When combined with the date and time of the measurement, calibration information that is associated with each labeled source enables computation of the activity when the measurement was performed.

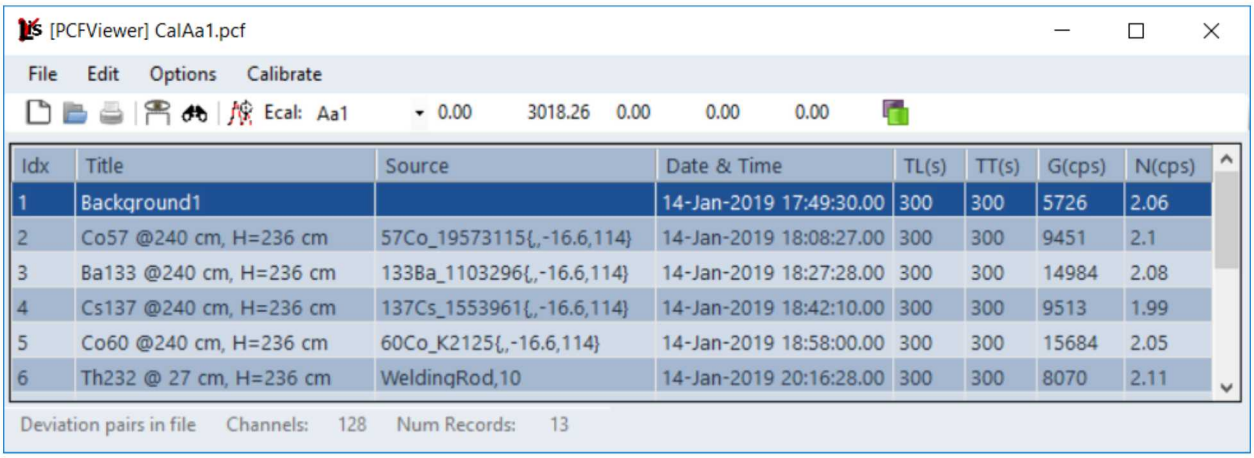

Idx	Title	Source	Date & Time	TL(s)	TT(s)	G(cps)	N(cps)
1	Background1		14-Jan-2019 17:49:30.00	300	300	5726	2.06
2	Co57 @240 cm, H=236 cm	57Co_19573115{,,-16.6,114}	14-Jan-2019 18:08:27.00	300	300	9451	2.1
3	Ba133 @240 cm, H=236 cm	133Ba_1103296{,,-16.6,114}	14-Jan-2019 18:27:28.00	300	300	14984	2.08
4	Cs137 @240 cm, H=236 cm	137Cs_1553961{,,-16.6,114}	14-Jan-2019 18:42:10.00	300	300	9513	1.99
5	Co60 @240 cm, H=236 cm	60Co_K2125{,,-16.6,114}	14-Jan-2019 18:58:00.00	300	300	15684	2.05
6	Th232 @ 27 cm, H=236 cm	WeldingRod,10	14-Jan-2019 20:16:28.00	300	300	8070	2.11

Figure 1. Header information contained in the calibration spectra file.

3. DRF REFINEMENT AT A SINGLE POSITION

3.1. PVT Portals

The accuracy of computed spectra obtained by the characterization procedure outlined in Section 2 is sufficient for most applications. Exceptions would be when computed spectra must be accurate, but the detector response exhibits characteristics not described sufficiently by the response function. The refinement method is entirely empirical, so users are strongly advised to obtain the best characterization using the normal detector characterization method before refinement so that characterization extrapolates well to gamma-ray energies that are not represented in the calibration source set. Figure 2 compares measured calibration spectra for a PVT portal with calculations based on GADRAS Versions 18.7.9 and 18.8.2. The accuracy of computed spectra is reasonably good with both versions except in the regions below 100 keV. No gamma rays with significant yield are emitted in these regions, and the intensities are too high to be associated with scattered photons. Although these spectral features are not observed for other types of detectors, most PVT portals exhibit similar characteristics. While differences between measured and computed spectra may not appear to be severe when viewing the spectra overall, some analysis algorithms utilize spectral regions extending to the lowest energies, so the computational errors could be important for performance evaluations. Chi-square differences that are displayed in the upper-right corner of each plot show significant improvements the computational accuracy obtained with Version 18.8.2.

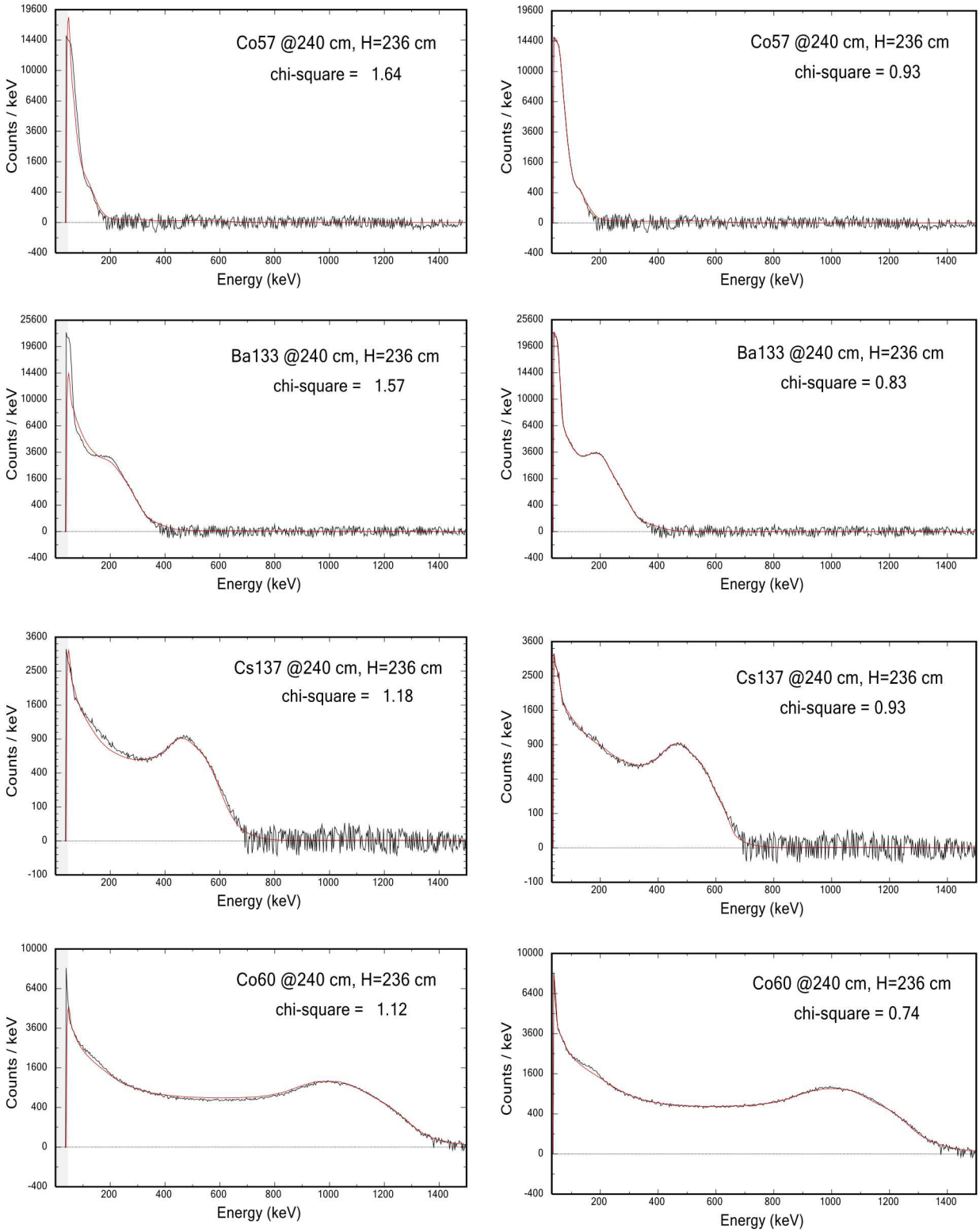

Figure 2. The left column compares measured spectra (black) for a PVT portal with computed spectra based on GADRAS Version 18.7.9 (red) and the right column shows results obtained after refining the response using Version 18.8.2.

The empirical refinement method is an advanced user feature that will not be applicable for most sensor characterizations. Directing GADRAS to perform the empirical refinement requires creation of a file named "DetectorUnique.gadras", which is not normally present in a detector folder. The example file shown in Figure 3 declares that refinement will be performed at one angle (0° relative to the detector normal) and four energies: 122, 356, 661, and 1332 keV. It also associates ^{57}Co, ^{133}Ba, ^{137}Cs, and ^{60}Co as the calibration sources that are paired with these energies. This example specifies that the continua will be adjusted in 16 spectral segments extending from zero to slightly more than the full gamma-ray energy. When "DetectorUnique.gadras" is present, the detector edit form displays an <*Empirical Refinement*> command button. No additional information is necessary because the detector should have been characterized already. "Cal.dat" and properly labeled calibration spectrum files, like the one shown in Figure 1, should already exist. The empirical refinement algorithm reads spectrum file names and indices contained in "Cal.dat", then reads title information in the calibration files to associate spectra with energy mesh points for the empirical parameters. The refinement method is automated and executes in a few minutes or less. The output, which is appended to "DetectorUnique.gadras", contains a series of scalars that are applied to photopeaks and continua regions. Users can also edit these files manually.

```
Version =          2.0
AngleCount =       1
Angles =           0.0
EnergyCount =      4
Energies =         122    356    661    1332
SourceNames =      CO57  BA133 CS137 CO60
SegmentCount =     16
Data =
```

Figure 3. Content of an initial "DetectorUnique.gadras" file.

3.2. Detectors Coupled with SiPM

All scintillators exhibit nonlinearity of the pulse height versus gamma-ray energy to varying extents, which is normally accommodated by calibration procedures that define polynomial terms or deviations from linearity at a series of mesh points. Nonlinearity of the detector response also leads to subtle variations of the spectral shape resulting from the varying distributions of secondary electrons following gamma-ray interactions. For example, photopeaks can be produced either by complete absorption of the incident gamma ray or from a series of Compton scattering events before the final photoelectric absorption. Variations in the way the energy is partitioned lead to shifts in Compton edges and escape peaks relative to the energies that would be observed for a detector with linear response. GADRAS applies automatic compensation for these effects based on the nominal performance for scintillators attached to photomultiplier tubes (PMT). Detectors coupled with SiPM exhibit greater nonlinearities and more variability from one unit to the next, at least for the current generation of SiPM devices. Therefore, SiPM technology imposes the need to characterize spectral effects that are unique to individual detectors.

Figure 4 compares a spectrum measured when a D3S detector (small CsI crystal coupled with SiPM) was exposed to a ^{232}U source with computed spectra. Without compensation, the computed

locations of escape peaks and the Compton edge associated with the 2614-keV gamma ray are all shifted relative to the measurement. These differences are eliminated following empirical refinement. The intensities of escape peaks are also adjusted, but the cause of this discrepancy is likely caused by an inadequacy of the GADRAS DRF rather than being specifically associated with SiPM. Figure 5 shows the content of the "DetectorUnique.gadras" file after the refinement is performed. The setup information is essentially the same as the setup for the PVT. When the response is refined for detectors that exhibit photopeaks, an attempt is made to adjust the peak shape parameters. In this case, none of the shape parameters were adjusted because the original fit was sufficiently accurate (parameters in this file represent scalars for the peak widths and additive values for the skew parameters). Columns labeled "dEdge", 'dSE", and "dDE" represent shifts in units of keV for the Compton edge, single escape peak, and double escape peak, respectively. Columns labeled "iSE", "iDE", and "iFlu" represent intensities of escape peaks and fluorescence x-rays relative to nominal computed values for these peaks. Empirical adjustments are not computed for gamma-rays with energies less than 2000 keV because these features are not produced by lower-energy gamma rays.

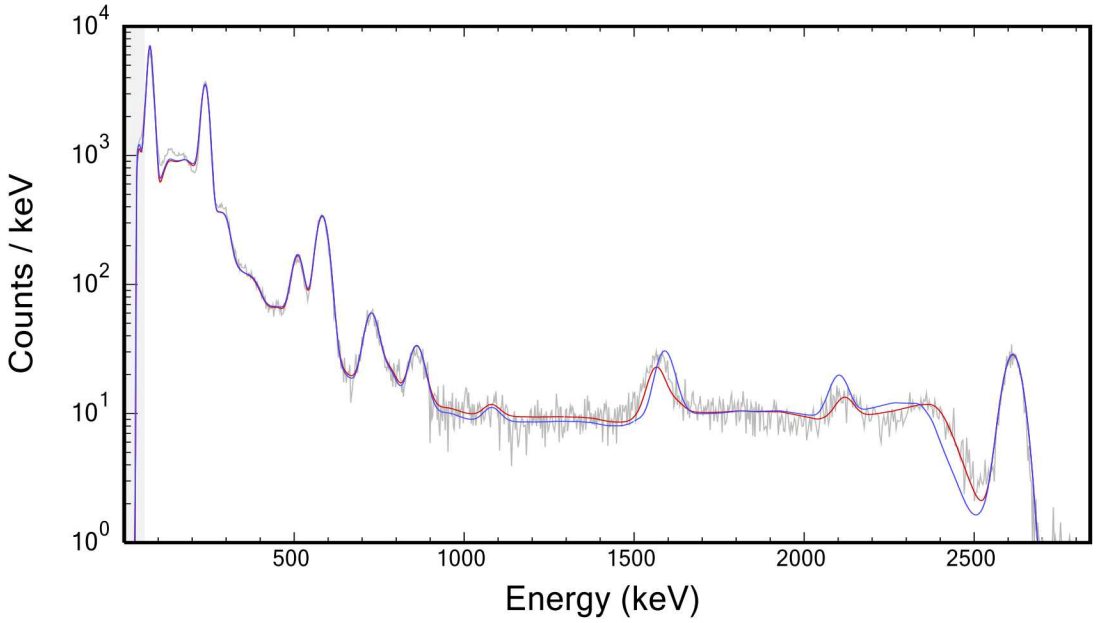

Figure 4. The measured spectrum (gray) for a ^{232}U measured by a D3S detector is compared with computed spectrum using GADRAS Version 18.8.2 (red) and a spectrum obtained without empirical refinement (blue).

```
Version =         2.0
AngleCount =      1
Angles =          0.0
EnergyCount =     5
Energies =        81    356    661   1332   2614
SourceNames =     BA133 BA133 CS137 CO60  U232
SegmentCount =    4
Data =
 Energy  Width  SkewL ExtenL  SkewH ExtenH  dEdge    dSE    dDE    iSE    iDE   iFlu  Peak(...
   81.0   1.00   0.00   0.00   0.00   0.00   0.00   0.00   0.00   1.00   1.00   1.00  0.987...
  356.0   1.00   0.00   0.00   0.00   0.00   0.00   0.00   0.00   1.00   1.00   1.00  0.973...
  661.0   1.00   0.00   0.00   0.00   0.00  -1.41   0.00   0.00   1.00   1.00   1.00  0.992...
 1332.0   1.00   0.00   0.00   0.00   0.00  -3.38   0.00   0.00   1.00   1.00   1.00  0.809...
 2614.0   1.00   0.00   0.00   0.00   0.00  50.36  16.97 -22.66   0.44   0.67   1.00  0.991...
```

Figure 5. Content of "DetectorUnique.gadras" file after performing empirical refinement for a D3S detector.

4. REFINING THE ANGULAR DEPENDENCE

Until recently, the angular dependence of the DRF was ignored because sources were assumed to be located on the detector axis or variations with angle were small over the limited ranges for which the detectors were designed to operate. The importance of angular effects depends on how the calculations are applied. For example, the integrated spectrum that is accrued while a source passes through a portal is similar to the spectrum at the point of closest approach because the count rate is maximized while the source is near the detector. However, when compared with the average, spectra that are segmented as functions of time or displacement may differ considerably as the distance from the detector increases, and evaluating the performance of analysis algorithms can be misleading without taking these variations into consideration. This section describes two cases where the angular dependence of the DRF are important.

4.1. Gross Spectrometers

Attenuation and scattering of gamma rays that strike the sides of detectors are based on crude descriptions of the surrounding material, which is represented by an effective atomic number, areal density, and length. The description does not contain provisions for differing types or thicknesses of materials that may extend to different lengths along the sides and front of the detector element. Consequently, it is not surprising to find that the normal set of characterization parameters cannot replicate peak intensities and continua shapes for all positions and gamma-ray energies. Plots displayed in Figure 6 compare measured and computed spectra at 0° and 26° relative to the detector axis for a collimated HPGe detector with a field-of-view of approximately 60°. The plot on the left shows that the continuum magnitudes differ by as much as 50% based on the nominal description of the collimator. Although differences in peak intensities are not as apparent with this resolution, their magnitudes also differ by a similar amount. The plot on the right shows the same comparison after empirical refinement. The photopeak intensities are in nearly perfect agreement and the continua are improved substantially. Empirical refinement is achieved using the same type of "DetectorUnique.gadras" file as discussed previously except the "AngleCount" and "Angles =" lines are augmented to represent all positions where characterization spectra were measured (see Figure 7). Additional title information that is required in the calibration spectrum file is represented by the angle followed by the string "degrees". The angles must be exactly the same as angles listed in "DetectorUnique.gadras". Additional information in the title block, such as the offset in inches,

which was added for record keeping purposes, is not used nor does it interfere with empirical refinement.

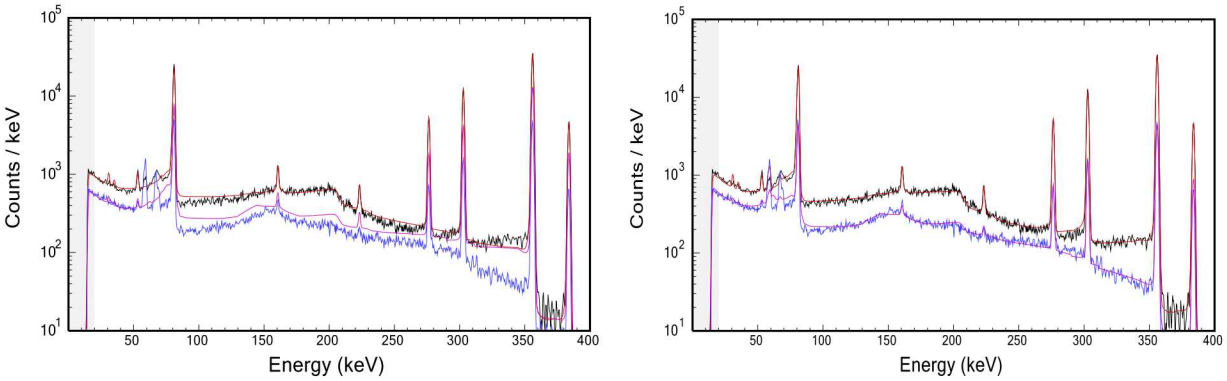

Figure 6. Measured spectra for ^{133}Ba directly in front of the detector (0°) and the same source at 26° are represented by the black and blue spectra, respectively. The plot on the left shows computed spectra (red and magenta) with no refinement. The plot on the right compares the measurements with computed spectra after empirical refinement.

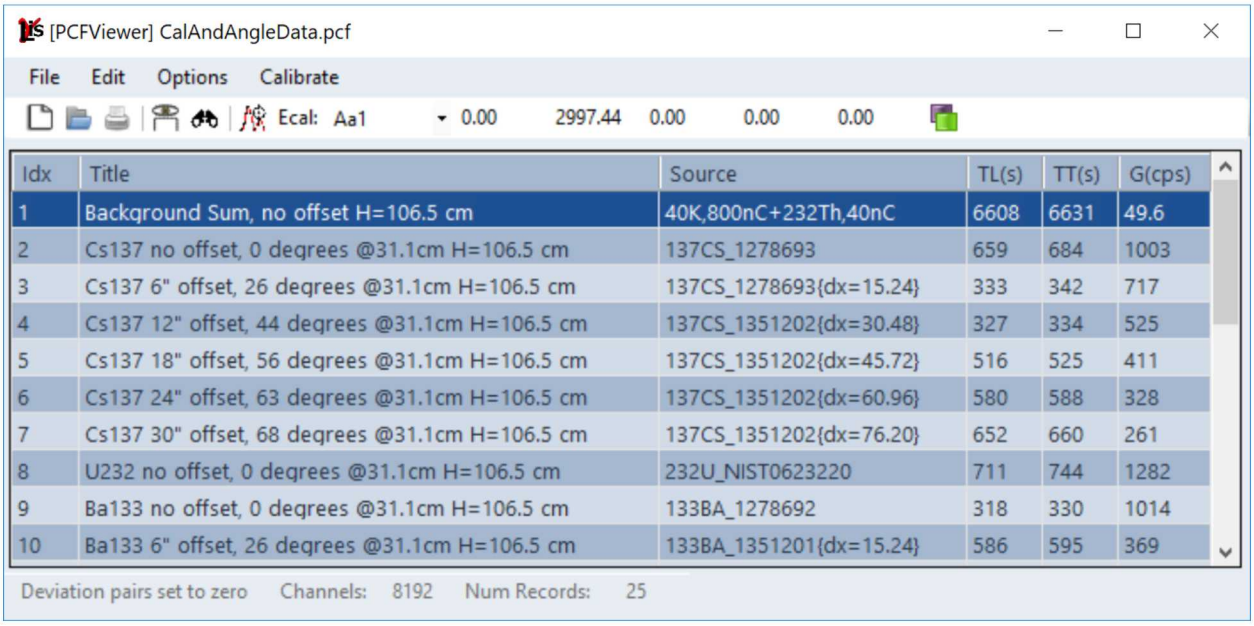

Idx	Title	Source	TL(s)	TT(s)	G(cps)
1	Background Sum, no offset H=106.5 cm	40K,800nC+232Th,40nC	6608	6631	49.6
2	Cs137 no offset, 0 degrees @31.1cm H=106.5 cm	137CS_1278693	659	684	1003
3	Cs137 6" offset, 26 degrees @31.1cm H=106.5 cm	137CS_1278693{dx=15.24}	333	342	717
4	Cs137 12" offset, 44 degrees @31.1cm H=106.5 cm	137CS_1351202{dx=30.48}	327	334	525
5	Cs137 18" offset, 56 degrees @31.1cm H=106.5 cm	137CS_1351202{dx=45.72}	516	525	411
6	Cs137 24" offset, 63 degrees @31.1cm H=106.5 cm	137CS_1351202{dx=60.96}	580	588	328
7	Cs137 30" offset, 68 degrees @31.1cm H=106.5 cm	137CS_1351202{dx=76.20}	652	660	261
8	U232 no offset, 0 degrees @31.1cm H=106.5 cm	232U_NIST0623220	711	744	1282
9	Ba133 no offset, 0 degrees @31.1cm H=106.5 cm	133BA_1278692	318	330	1014
10	Ba133 6" offset, 26 degrees @31.1cm H=106.5 cm	133BA_1351201{dx=15.24}	586	595	369

Figure 7. Title information contained in the calibration spectra file must contain the angular displacement when the data are to be used to refine the DRF as a function of angle.

Utilization of the empirical DRF refinement capabilities to enhance the DRF at angular offsets, additional measurements must be taken at different angles. The angular range and intervals at which measurements should be performed will vary by detector system.

4.2. Imaging Spectrometers

GADRAS incorporates provisions for characterization of Compton cameras and coded aperture imagers. Imagers present a new set of challenges because the DRF varies with the angular displacement between the actual source position and the spatial region associated with the spectral computation. Characterization of imaging detectors is documented elsewhere [3,4]. The capability for imaging sensors is discussed in this document because after recognizing the similar needs for empirical refinement, the interfaces were combined so that "DetectorUnique.gadras" is now applied for all detector types. However, title fields in calibration spectrum files are slightly different because all of the angular information is collected simultaneously when imaging detectors are characterized. As shown in Figure 8, the title fields specify a series of azimuthal angles. Data represented in this file define spectra associated with a concentric bull's eye pattern centered about the source location. The series of angles specified in the "DetectorUnique.gadras" file must be exactly equal to the midpoints of the angular groups in the spectra file. Figure 9 compares computed spectra for a ^{137}Cs source in three acceptance angles with measurements that were acquired with a CZT-based Compton camera.

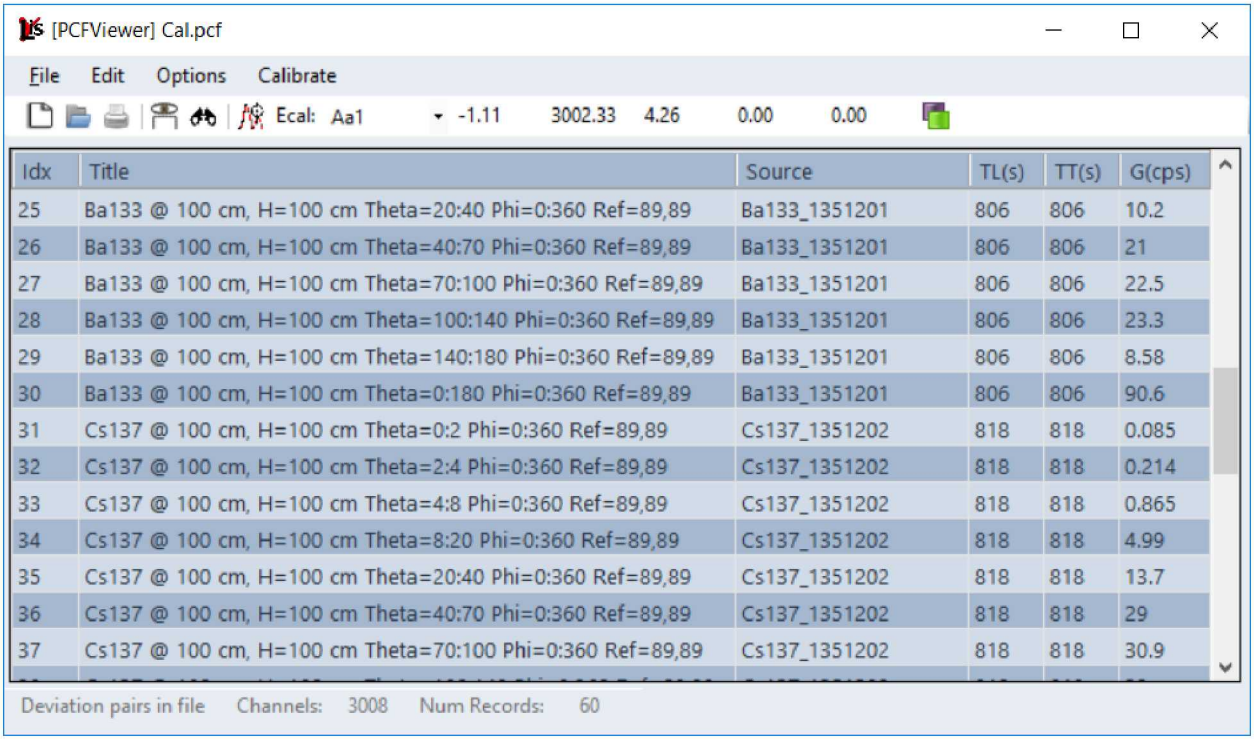

Idx	Title	Source	TL(s)	TT(s)	G(cps)
25	Ba133 @ 100 cm, H=100 cm Theta=20:40 Phi=0:360 Ref=89,89	Ba133_1351201	806	806	10.2
26	Ba133 @ 100 cm, H=100 cm Theta=40:70 Phi=0:360 Ref=89,89	Ba133_1351201	806	806	21
27	Ba133 @ 100 cm, H=100 cm Theta=70:100 Phi=0:360 Ref=89,89	Ba133_1351201	806	806	22.5
28	Ba133 @ 100 cm, H=100 cm Theta=100:140 Phi=0:360 Ref=89,89	Ba133_1351201	806	806	23.3
29	Ba133 @ 100 cm, H=100 cm Theta=140:180 Phi=0:360 Ref=89,89	Ba133_1351201	806	806	8.58
30	Ba133 @ 100 cm, H=100 cm Theta=0:180 Phi=0:360 Ref=89,89	Ba133_1351201	806	806	90.6
31	Cs137 @ 100 cm, H=100 cm Theta=0:2 Phi=0:360 Ref=89,89	Cs137_1351202	818	818	0.085
32	Cs137 @ 100 cm, H=100 cm Theta=2:4 Phi=0:360 Ref=89,89	Cs137_1351202	818	818	0.214
33	Cs137 @ 100 cm, H=100 cm Theta=4:8 Phi=0:360 Ref=89,89	Cs137_1351202	818	818	0.865
34	Cs137 @ 100 cm, H=100 cm Theta=8:20 Phi=0:360 Ref=89,89	Cs137_1351202	818	818	4.99
35	Cs137 @ 100 cm, H=100 cm Theta=20:40 Phi=0:360 Ref=89,89	Cs137_1351202	818	818	13.7
36	Cs137 @ 100 cm, H=100 cm Theta=40:70 Phi=0:360 Ref=89,89	Cs137_1351202	818	818	29
37	Cs137 @ 100 cm, H=100 cm Theta=70:100 Phi=0:360 Ref=89,89	Cs137_1351202	818	818	30.9

Figure 8. This screen capture summarizes records in a calibration spectrum file for a Compton camera.

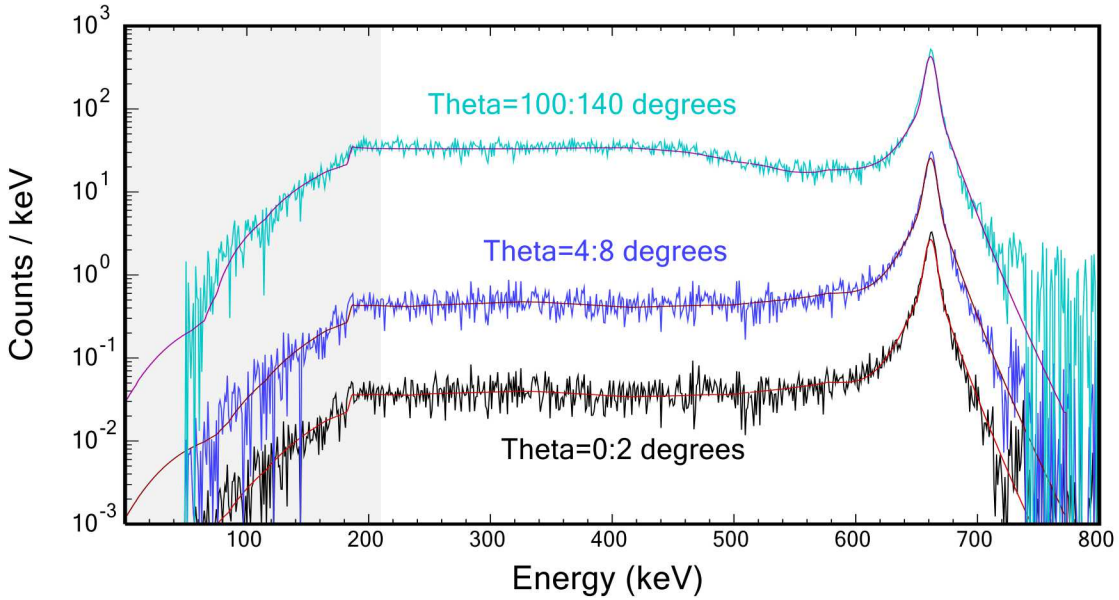

Figure 9. Computed spectra for a ^{137}Cs source in three acceptance angles are compared with measurements that were acquired with a CZT-based Compton camera. The low-energy region displays a gray background to indicate that this region is not weighted when spectra are analyzed.

5. SUMMARY AND CONCLUSIONS

GADRAS Version 18.8.2 includes provisions for empirical refinement of the DRF. The expectation is that the normal characterization procedures will be applied for most detectors and that refinement will only be performed in exceptional circumstances, such as those described in this document. When characterization data is sufficient to support empirical refinement, this capability enables almost perfect replication of spectral characteristics as functions of gamma-ray energy and angular displacement.

REFERENCES

1. D.J. Mitchell, “Radiation Detector Characterization Requirements for GADRAS,” Sandia National Laboratories Report SAND2015-2920 TR, October 27, 2014.
2. M.W. Enghauser, “GADRAS-DRF Detector Response Function Characterization Training Aid,” Sandia National Laboratories Report SAND2017-9971 (UUR), August 2017.
3. D.J. Mitchell and S.M. Horne, “Characterization of Gamma-Ray Imagers Using GADRAS”, Sandia National Laboratories Report SAND2018-5749 (June 2018).
4. D.J. Mitchell, S.M. Horne, S. O’Brien, and G.G. Thoreson, “Directional Unfolded Source Term (DUST) for Compton Cameras,” Sandia National Laboratories Report SAND2018-2358, March 2018.

DISTRIBUTION

Email—External

Name	Company Email Address	Company Name
John Blackadar	John.Blackadar@hq.dhs.gov	DHS/CWMD
Chris Blessinger	blessingercs@ornl.gov	ORNL
Willy Kaye	Willy@h3dgamma.com	H3D
Michael Koehl	Michael.Koehl@nnsa.doe.gov	DOE/NNSA/NA-22
Marc Klasky	mklasky@lanl.gov	LANL
Robert Feuerbach	Robert.Feuerbach@jhuapl.edu	APL
Brian Fisher	Brian.Fisher@jhapl.edu	APL
Greg Slovik	Gregory.Slovik@hq.dhs.gov	DHS/CWMD

Email—Internal

Name	Org.	Sandia Email Address
Mike Enghauser	6634	mwengha@sandia.gov
Ronald Farmer	5877	rfarmer@sandia.gov
Lee Harding	6634	lthard@sandia.gov
Steve Horne	6634	smhorne@sandia.gov
Dean Mitchell	6630	djmitch@sandia.gov
Sean O'Brien	6634	sobrien@sandia.gov
Chuck Rhykerd	6634	clrhyke@sandia.gov
Lisa Theisen	6634	ltheise@sandia.gov
Greg Thoreson	6634	ggthore@sandia.gov
Technical Library	01177	libref@sandia.gov

This page left blank

This page left blank

Sandia National Laboratories

Sandia National Laboratories is a multimission laboratory managed and operated by National Technology & Engineering Solutions of Sandia LLC, a wholly owned subsidiary of Honeywell International Inc. for the U.S. Department of Energy's National Nuclear Security Administration under contract DE-NA0003525.